Review

Cell Culture and Animal Models of Nanoparticle Toxicity on the Airway Barrier

Claire E Lee and Fariba Rezaee *

Posted Date: 24 June 2024

doi: 10.20944/preprints202406.1674.v1

Keywords: airway epithelial cells; apical junctional complex; tight junction; adherens junction; nanoparticles; epithelial barrier dysfunction; permeability; inflammation; oxidative stress.

 doi:10.20944/preprints202406.1674.v1

Review

Cell Culture and Animal Models of Nanoparticle Toxicity on the Airway Barrier

Claire E. Lee [1,2] and Fariba Rezaee [1,3,*]

[1] Department of Inflammation and Immunity, Lerner Research Institute, Cleveland Clinic Foundation, Cleveland, Ohio, U.S.A.
[2] Case Western Reserve University, Cleveland, Ohio, U.S.A.
[3] Center for Pediatric Pulmonary Medicine, Cleveland Clinic Children's, Cleveland, Ohio, U.S.A.
* Correspondence: rezaeef@ccf.org

Abstract: The production of nanoparticles has recently surged due to their varied applications in biomedical, pharmaceutical, textile, and electronic sectors. However, this rapid increase in nanoparticle manufacturing has raised concerns about environmental pollution, particularly due to their potential adverse effects on human health. Among the various concerns, inhalation exposure to nanoparticles poses significant risks, especially affecting the respiratory system. Airway epithelial cells play a crucial role as the primary defense against inhaled particulate matter and pathogens. Studies have shown that nanoparticles can disrupt the airway epithelial barrier, triggering inflammatory responses, generating reactive oxygen species, and compromising cell viability. However, our understanding of how different types of nanoparticles specifically impact the airway epithelial barrier remains limited. To investigate nanoparticle-induced cellular responses and barrier dysfunction, both in vitro cell culture models and in vivo murine models are commonly utilized. In this review, we discuss the methodologies frequently employed to assess nanoparticle toxicity and barrier disruption. Furthermore, we analyze and compare the distinct effects of various nanoparticle types on the airway epithelial barrier. By elucidating the diverse responses elicited by different nanoparticles, we aim to provide insights that can guide future research endeavors in assessing and mitigating the potential risks associated with nanoparticle exposure.

Keywords: airway epithelial cells; apical junctional complex; tight junction; adherens junction; nanoparticles; epithelial barrier dysfunction; permeability; inflammation; oxidative stress

1. Introduction

Nanoparticle manufacturing has applications in numerous fields such as agriculture, medicine, cosmetics, environmental monitoring, and drug development [1,2]. Notably, nanoparticles like TiO_2 are used in food additives and coatings to preserve the shelf life of fruits [3–5]. Nanoparticles typically range from 1-100 nm in diameter and exhibit varied physicochemical properties depending on their size, elemental composition, and specific crystal structure [6,7]. They can block UV radiation by absorbing, scattering, and reflecting both short and long wavelengths of ultraviolet light [8]. Nanoparticles have high surface-to-volume ratios which enhances their thermal conductivity and catalytic activity [9]. Metal nanoparticles have become a popular material used for wound healing, tumor targeting, and other biomedical approaches [10]. Metal nanoparticles predominantly comprise pure metal and metal oxide nanoparticles. Pure metal nanoparticles include AgNPs, AuNPs, and CoNPs. These compounds have enhanced thermodynamic stability and antimicrobial properties [11–13]. Similarly, metal oxide nanoparticles like TiO_2-NPs, ZnO-NPs, Al_2O_3-NPs, and CuO-NPs are utilized to inhibit the transmission of pathogens [14]. Metal oxides also have optical properties such as UV absorption and photoluminescence [15]. However, inhalation of metal nanoparticles has been reported to cause detrimental effects such as lung inflammation and carcinogenesis [16]. The mechanisms causing these adverse responses involve the release of radical oxygen species and

 doi:10.20944/preprints202406.1674.v1

penetration of the airway barrier by metal ions. Additionally, nonmetal nanoparticles like SiO_2-NPs and GONPs contribute to airway hypersensitivity, fibrogenic responses, and oxidative stress [17].

Airway epithelial cells (AECs) play a crucial role in understanding the interactions between metal or nonmetal nanoparticles and the respiratory tract. These cells are the primary targets for pathogens and harmful particles via inhalation [18–20]. Alongside AECs, intercellular apical junctional complexes (AJCs) comprising tight junctions (TJs) and adherens junctions (AJs), are responsible for junction assembly/disassembly and interactions with nearby cells [21,22]. Together, the barrier function and mucociliary clearance presented by AECs, as well as the maintenance of barrier integrity by AJCs, serve as a dynamic defense structure [23]. Nanoparticles cause dysfunction and have detrimental impact to the AJCs by increasing permeability of the epithelial barrier [24,25] (**Figure 1**). Due to their small size, nanoparticles deposit deep in the lung, with increasing deposition efficiencies as their diameter decreases [26]. Common manifestations of nanoparticle exposure include fibrosis and chronic inflammation in addition to epithelial injury [27].

Figure 1. Exposure to nanoparticles cause adverse cellular responses.

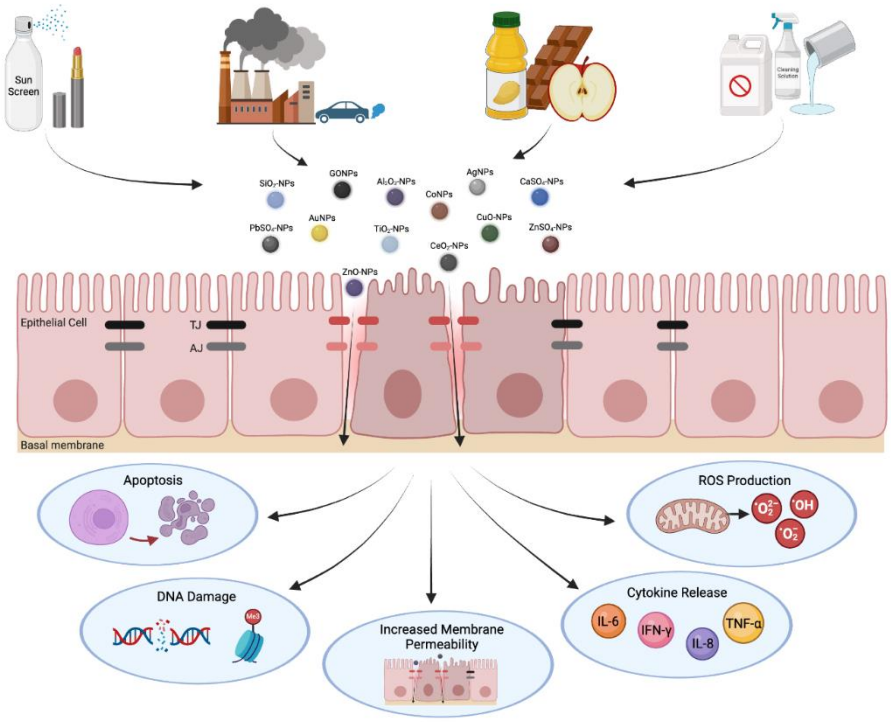

Figure 1. Exposure to nanoparticles cause adverse cellular responses. Inhalation of nanoparticles occurs in various applications, such as the use of cosmetics and cleaning products, occupational exposure, and food additives. When exposed, nanoparticles can penetrate the epithelial barrier and cause AJC dysfunction. The disruption of TJ and AJ structures leads to harmful cellular responses, including cell death, genetic alterations, inflammation, and oxidative stress. This figure was created with BioRender.com.

Despite the growing industry of nanomaterials, limited knowledge exists regarding nanoparticle toxicity and the associated risks to the respiratory tract. Specifically, there is a lack of comparative studies on different types of nanoparticles and their impact on the airway epithelial barrier. Past studies have used cell culture and murine models as in vitro and in vivo methods, respectively, to examine nanoparticle-induced inflammatory and cellular responses. Using primary or immortalized cell lines can provide insights into nanoparticle uptake and the functional activity of AECs [28,29]. Similarly, experiments on mice and rats can offer a more representative model for assessing structural and functional changes in the lung [30]. Both model types encounter challenges such as inconsistent cell morphology and differences in lung anatomy between mice/rats and humans [31,32]. However, they provide valuable understanding into the effects of nanoparticles on the airway epithelial barrier at a cellular level. In this review, we discuss various cell culture and murine models that investigate

 doi:10.20944/preprints202406.1674.v1

the impact of common metal and non-metal nanoparticles on AECs. We focus on the cellular responses of primary and immortalized cell lines, as well as mice and rat models. We reveal the specific mechanisms by which nanoparticles disrupt the airway epithelial barrier and compare the effects of various nanoparticle types. This insight will benefit future studies selecting the appropriate experimental model based on the nanoparticle of interest.

2. Cell Culture Studies on Airway Cells:

Cultured airway epithelial cells retain certain cell characteristics, which are valuable for studying structural and functional changes of the airway barrier induced by inhalation of harmful particulate matter and inflammatory responses [33]. Cell culture models provide a simplified, controlled environment that allows for different cell lines to be studied for nanoparticle toxicity in the epithelial airway (**Table 1**). Here, we focus on the well-studied 16HBE14o-, A549, Calu-3, and NHBE cell lines.

Table 1. Nanoparticle impact on AJC barrier and cellular responses using cell culture models.

Cell Culture Model	Nanoparticle type	Nanoparticle Concentration	Impact on Barrier Function	Cellular Responses	Reference
16HBE14o- human bronchial epithelial cells (16HBE)	TiO_2-NPs	10, 25, 50, 75, and 100 μg/mL	↓ TEER ↑ Permeability	↑ ROS production ↑ Viral infection ↑ Interleukins, TNF-α, IFN-γ, CCL-3, GM-CSF release	[40]
		100 μg/mL	↓ TEER ↑ Permeability	-	[41]
		0.1, 1, 10 and 100 μg/mL	-	↑ ROS production ↑ Cytotoxicity ↓ Cell viability ↓ DNA methylation	[42]
		3, 15 and 75 μg/cm²	-	↑ ROS production ↑ GM-CSF, IL-6 and IL-8 release ↑ Cytotoxicity	[43]
		20 μg/cm²	-	↑ ROS production ↑ Apoptosis ↑ DNA fragmentation ↓ Lysosome stability	[78]
		40 μg/mL	-	↓ Cell viability ↓ Cell migration ↑ Apoptosis ↑ Oxidative stress	[44]

 doi:10.20944/preprints202406.1674.v1

SiO_2-NPs			↑ IL-6, IL-8, TNF-α release	
	3, 15 and 75 μg/cm²	-	↑ ROS production ↑ GM-CSF, IL6 and IL8 release ↑ Cytotoxicity	[43]
ZnO-NPs	1, 5, 25 and 50 μg/mL	-	↑ ROS production ↓ Mitochondrial membrane potential ↑ Apoptosis	[45]
TiO_2-NPs	40 μg/mL	-	↑ Endocytosis of aggregates	[60]
	1, 10 and 50 μg/mL	-	↑ ROS production ↓ Cell viability ↑ Cytotoxicity ↑ Apoptosis	[50]
	25, 50, 100, and 200 μg/mL	-	↑ Cytotoxicity ↑ Apoptosis ↑ DNA strand breaks ↓ Cell viability ↓ Mitochondrial membrane potential	[51]
	0.1, 1, 10 and 100 μg/mL	-	↑ ROS production ↑ Cytotoxicity ↓ Cell viability ↓ DNA methylation	[42]
	3, 15 and 75 μg/cm²	-	↑ ROS production ↑ IL-6 release ↑ Cytotoxicity	[43]
	5–500 μg/mL	-	↑ ROS production ↑ IL-8 release ↓ Cell viability	[79]
AgNPs	25, 50, 100 or 200 μg/mL	-	↑ ROS production ↓ Cell viability ↓ Mitochondrial membrane potential ↑ Apoptosis	[52]
	5 μg/mL		↑ IL-1β, IL-6, IL-8, TNF-α release	[58]

 doi:10.20944/preprints202406.1674.v1

Human A549 adenocarcinoma cells (A549)		*Co-culture with U937	-	↑ ROS production *(less than A549 alone)*	
		0.05-0.8 μg/cm²	No change	↑ ROS production	[80]
	AuNPs	0.05-0.8 μg/cm²	No change	↑ ROS production	[80]
	SiO_2-NPs	10, 50, 100, and 250 μg/mL	-	↓ Cell viability ↑ ROS production ↓ Mitochondrial membrane potential	[54]
		3, 15 and 75 μg/cm²	-	↑ ROS production ↑ GM-CSF, IL-6, IL-1β, IL-8 release ↑ Cytotoxicity	[43]
		10, 50, 100, 200, 300, 400 μg/mL	-	↓ Cell viability ↑ Necrosis ↑ NP accumulation and retention	[76]
	ZnO-NPs	5, 10, 15, 20 μg/mL	-	↓ Cell viability ↑ ROS production ↓ Mitochondrial membrane potential	[53]
	GONPs	0.05, 0.5, 5, 50, 100 μg/mL	-	↑ Necrosis ↑ Apoptosis ↓ Cell viability	[77]
	$CaSO_4$-NPs	10-320 μg/mL	-	↑ ROS production	[59]
	$ZnSO_4$-NPs	10-320 μg/mL	-	↑ ROS production ↑ DNA damage ↑ Cytotoxicity ↑ JNK regulation	
	$PbSO_4$-NPs	10-320 μg/mL	-	↑ ROS production	
		1 μg/cm²	No change	No changes in cell viability, barrier integrity, or cytokine release	[64]

 doi:10.20944/preprints202406.1674.v1

Cultured human airway epithelial cells (Calu-3)	TiO_2-NPs	0.25-2 mM	No change	No changes in cell viability or cytotoxicity	[65]
		5 and 10 μg/cm²	↑ TEER	↑ NP internalization	[66]
	SiO_2-NPs	5 and 10 μg/cm²	↑ TEER	↑ NP internalization	[66]
		100 μg/mL	-	↑ ROS production ↑ Cytotoxicity ↑ Apoptosis ↑ IL-6, IL-8 release	[67]
	ZnO-NPs	0.25-2 mM	↓ TEER	↓ Cell viability	[65]
Normal human bronchial epithelial cells (NHBE)	TiO_2-NPs	20 μg/cm²	-	↑ ROS production ↑ Apoptosis ↑ DNA fragmentation ↓ Lysosome stability	[78]
		10, 25, 50, 75, and 100 μg/mL	↓ TEER ↑ Permeability	-	[40]
		5–500 μg/mL	-	↑ ROS production (weak) ↑ IL-6, IL-1β, G-CSF, VEGF release ↓ Cell viability	[79]
	SiO_2-NPs	10, 50, 100, 200, 300, 400 μg/mL	-	↓ Cell viability ↑ Necrosis ↑ NP accumulation and retention	[76]
	GONPs	0.05, 0.5, 5, 50, 100 μg/mL	-	↑ Necrosis ↑ Apoptosis ↓ Cell viability ↑ Oxidative stress	[77]
	AgNPs	0.05-0.8 μg/cm²	-	↑ LDH release ↓ Cell viability ↑ ROS production (weak)	[80]
	AuNPs	0.05-0.8 μg/cm²	-	↑ LDH release ↓ Cell viability	[80]

 doi:10.20944/preprints202406.1674.v1

							↑ ROS production (weak)

List of abbreviations: AgNPs, silver nanoparticles; AuNPs, gold nanoparticles; $CaSO_4$-NPs, calcium sulfate nanoparticles; CCL-3, macrophage inflammatory protein 1-α; G-CSF, granulocyte colony stimulating factor; GM-CSF, granulocyte macrophage colony stimulating factor; GONPs, graphene oxide nanoparticles; IL-1β, interleukin-1 beta; IL-6, interleukin-6; IL-8, interleukin-8; IFN-γ, interferon gamma; JNK, jun N-terminal kinase; LDH, lactate dehydrogenase; $PbSO_4$-NPs, lead sulfate nanoparticles; ROS, reactive oxygen species; SiO_2-NPs, silicon dioxide nanoparticles; TiO_2-NPs, titanium dioxide nanoparticles; TNF-α, tumor necrosis factor alpha; VEGF, vascular endothelial growth factor; ZnO-NPs, zinc oxide nanoparticles; $ZnSO_4$-NPs, zinc sulfate nanoparticles; ↓, decreased; ↑, increased; -, not determined.

2.1. 16. HBE14o- (16HBE) Human Bronchial Epithelial Cells

The 16HBE14o- (16HBE) cell line is a commonly used in vitro model for airway barrier properties and was derived from human bronchial epithelium immortalized with SV40 plasmid [34, 35]. 16HBE cells have stable TJ morphology and have been shown to be suitable for assessing the airway epithelium's permeability function [36,37]. TJs are located in the apical region of the AJC and create a "fence" between adjacent cells [38]. This "fence" maintains selective permeability for proper exchange and paracellular transport of ions. When barrier disruption occurs, loss of permeability in the epithelial membrane causes uncontrolled, leaky airways [39]. In regards to barrier function, exposure of 16HBE cells to TiO_2-NPs has been shown to increase epithelial membrane permeability by decreasing transepithelial electrical resistance (TEER) [40]. For example, Lee et al. exposed 16HBE cells to 100 μg/mL of TiO_2-NPs for 48 hours [41]. They observed a significant decrease in TEER values which shows barrier dysfunction caused by increased permeability of the epithelial cell monolayers. Immunofluorescent labeling also exhibited disruption of TJ and AJ structures and reduced fluorescence intensity for cells exposed to TiO_2-NPs. Conversely, the authors did not find any changes in TJ and AJ protein levels. This indicates that TiO_2-NPs induced airway barrier disruption by facilitating disassembly of TJ and AJ proteins, rather than altering protein expression. In addition, due to the high reproducibility of 16HBE cells, this cell line has been widely used to examine the effect of nanoparticles on airway inflammatory responses and reactive oxygen species (ROS) production. For instance, it has been demonstrated that exposure of 16HBE cells to TiO_2-NPs increased intracellular ROS levels at 1-100 μg/mL. However, the cell viability mainly decreased at concentrations above 10 μg/mL [42]. Likewise, another study reported that TiO_2-NPs caused an increase in intracellular ROS production at concentrations of 15 and 37.5 μg/cm^2 [43]. Bao et al. found that SiO_2-NPs caused oxidative stress and promoted apoptosis in 16HBE cells [44]. The authors observed an increase in expression of Bax, a pro-apoptosis protein, and a decrease in Bcl-2 expression, an anti-apoptosis protein. Another study examined the impact of ZnO-NPs on the generation of ROS by utilizing 16HBE [45]. They showed that ZnO-NPs induced ROS generation and increased cell apoptosis by down-regulating the mRNA and protein expression of anti-apoptosis protein Bcl-2. Mitochondrial membrane potential also decreased following exposure to ZnO-NPs. In general, ZnO-NPs have been shown to have the most cytotoxic impact on 16HBE cells compared to TiO_2-NPs and SiO_2-NPs [46,47].

2.2. A549 Adenocarcinoma (A549) Cells

The A549 adenocarcinoma cell line (A549) was first obtained from a type II pneumocyte lung tumor and is used to represent alveolar type II cells in the cell culture models [48]. As such, A549 cells are an appropriate model for studying the impact of nanoparticles on the peripheral lung region [49]. Like 16HBE cells, the A549 cell line has shown increased intracellular ROS levels and apoptosis caused by TiO_2-NPs. Srivastava et al. exposed A549 cells to 5-50 μg/mL of TiO_2-NPs for 6-24 hours [50]. They found that 10-50 μg/mL of TiO_2-NPs significantly increased ROS production at all time points. Additionally, they saw an increase in the expression of apoptotic markers, P^{53}, P^{21}, and caspase-3, which confirms the upregulation of apoptosis. Furthermore, Wang et al. used higher TiO_2-

 doi:10.20944/preprints202406.1674.v1

NPs concentrations of 100-200 μg/mL on A549 cells [51]. They used quantitative real-time PCR (qRT-PCR) to measure the mRNA expression of apoptosis markers, caspase-3 and caspase-9. The study found a significant increase in the expression of both markers at all TiO_2-NP concentrations. Previous studies have shown other types of nanoparticles like AgNPs, ZnO-NPs, and SiO_2-NPs induce cytotoxicity in A549 cells as well. Chairuangkitti et al. assessed the adverse impact of AgNPs on A549 cells [52]. The authors found that A549 exposure to 100-200 μg/mL of AgNPs for 48 hours led to an increase in intracellular ROS levels. Also, they observed a 50% reduction in cell viability after 48-hour exposure to 200 μg/mL of AgNPs. A study by Zhuo et al. examined how ZnO-NPs caused cellular damage to A549 cells [53]. They showed a significant decrease in cell viability at 15-40 μg/mL of ZnO-NPs for 24 hours. Intracellular ROS production was seen to increase at 5-20 μg/mL concentrations, and this was thought to induce mitochondrial damage in A549 cells. Rafieepour et al. examined the effect of SiO_2-NPs on A549 cells [54]. This study exposed A549 cells to 10-250 μg/mL of SiO_2-NPs for 24 and 72 hours. The investigators showed an increase in intracellular ROS generation for all SiO_2-NP concentrations and a decrease in cell survival. Mitochondrial membrane potential was also shown to decrease, which is in agreement with the findings by Zhuo et al. Collectively, these studies show that exposure of A549 cells to TiO_2-NPs, AgNPs, ZnO-NPs, and SiO_2-NPs triggers ROS production and apoptosis.

Interestingly, a study by Ma et al. revealed that A549 cells were more sensitive to 25-nm-sized TiO_2-NPs than 16HBE cells [42]. The authors found that exposure to 1-100 μg/mL of TiO_2-NPs caused significant cytotoxicity in A549 cells after 24 hours. However, it took 48 hours for the same cytotoxic increase to occur in the 16HBE. In a similar study, Guadagnini et al. exposed A549 and 16HBE cells to 3-75 μg/cm^2 of TiO_2-NPs and SiO_2-NPs [43]. They showed that TiO_2-NPs and SiO_2-NPs generated cytotoxicity in A549 cells at lower doses and shorter exposure times than 16HBE cells.

A limitation of A549 cells is their lack of transepithelial resistance due to the absence of an intact TJ structure [55]. The TEER for A549 cells is generally less than 100 Ω×cm^2 [56,57], making it difficult to study barrier function. However, A549 cells are regularly used as a single monolayer or co-culture with other epithelial cell lines to measure oxidative stress and cell viability, among other cellular responses. For instance, Braun et al. co-cultured A549 cells with the U937, a human monocytic cell line, to examine the effects of AgNPs [58]. The cultures were exposed to 5 μg/mL of AgNPs for 24 hours. Compared to A549, monoculture, the co-culture had no change in cell viability, implying that the presence of U937 attenuated cytotoxicity caused by AgNPs. ROS production also decreased in the co-culture group compared to just A549 exposure to AgNPs. Furthermore, Könczöl et al. evaluated the impact of metal-sulfate nanoparticles on A549 cells [59]. In this study, A549 cells were exposed to 50 and 100 μg/cm^2 of $CaSO_4$-NPs, 1 and 10 μg/cm^2 of $ZnSO_4$-NPs, or 100 μg/cm^2 of $PbSO_4$-NPs for 24 hours. They found that only $ZnSO_4$-NPs induced concentration-dependent cytotoxicity. All the NPs were observed to cause oxidative stress, with $ZnSO_4$-NPs showing the most intracellular ROS production. Genotoxicity assays were used to demonstrate DNA damage caused by $ZnSO_4$-NPs, while $PbSO_4$-NPs and $CaSO_4$-NPs led to less DNA damage. The authors found that $ZnSO_4$-NPs activated c-Jun N-terminal kinase (JNK), a regulator of apoptosis that responds to extracellular and intracellular stress. In another study, Stearns et al. exposed A549 to 40 μg/mL of TiO_2-NPs for 3, 6, and 24 hours [60]. At every time point, they observed membrane-bound vacuoles that contained aggregates of TiO_2-NPs. However, no particles were seen to move paracellularly through the TJs. Rather, TiO_2-NPs were internalized through ingestion and appeared later in the vacuoles.

2.3. Cultured Human Airway Epithelial (Calu-3) Cells

The Calu-3 is a mucus-secreting cell line derived from a pulmonary adenocarcinoma patient [61]. Calu-3 cells possess TJ structures [62] and yield the highest TEER values compared to other bronchial epithelial cell lines like 16HBE, H292, and BEAS-2B [63]. Several studies show that nanoparticle exposure to Calu-3 monolayers does not affect barrier function, cell viability, or cytotoxicity. A study by Braakhuis et al. measured the effect of 500 μg/mL of TiO_2-NPs on Calu-3 cells [64]. The authors saw no changes in TEER or mitochondrial activity during the 24-hour exposure period. Similarly, Stuetz et al. exposed Calu-3 cells to 0.25 mM and 2 mM of TiO_2-NPs and ZnO-NPs

 doi:10.20944/preprints202406.1674.v1

for 24 hours [65]. They showed that only ZnO-NP exposure caused a decrease in cell viability and TEER at all concentrations. On the other hand, cytotoxicity was not significantly affected by either TiO_2-NPs or ZnO-NPs. Previous findings of Calu-3 exposure to SiO_2-NPs are not uniform either. For example, George et al. exposed Calu-3 to 5 and 10 μg/cm² of SiO_2-NPs and TiO_2-NPs for 24 hours [66]. In this study, SiO_2-NPs and TiO_2-NPs were translocated and internalized across Calu-3 monolayers without damaging epithelial integrity. The authors observed an increase in TEER rather than the usual decrease that reflects diminished barrier function. In contrast, a study by McCarthy et al. assessed the impact of different-sized SiO_2-NPs on Calu-3 cells [67]. They used 10-nm, 150-nm, and 500-nm-sized SiO_2-NPs at a concentration of 100 μg/mL for a 24-hour exposure period. 10-nm-sized SiO_2-NPs were found to induce cytotoxicity, apoptosis, and intracellular ROS generation in the Calu-3. However, SiO_2-NPs that were 150 and 500 nm did not have any toxic effects. These data suggest that Calu-3 cells respond differently depending on the type and composition of nanoparticles.

While many other lung epithelial cell lines, such as H441 and BEAS-2B, have been used in cell culture studies, we have decided to focus on 16HBE, A549, and Calu-3 cell lines. These are three of the most frequently used airway epithelial cell lines in nanoparticle toxicity studies. The Calu-3 and 16HBE are advantageous because they exhibit tight junctions [18]. Moreover, all three cell lines can be used to study drug metabolism in the airway epithelium [68,69].

2.4. Human Bronchial Epithelial (NHBE) Cells

In addition to immortalized cells, primary cells are beneficial because they are more physiologically representative of the epithelial airway [70]. The challenges of using primary cells include their short lifespan, difficulty in isolating cells, and variability between cell samples [71]. However, normal human bronchial epithelial (NHBE) cells have well-established TJs [72] and are frequently used to study respiratory diseases like influenza and RSV [73–75]. Other studies have used NHBE cells in conjunction with an immortalized cell line to compare the toxic effects of nanoparticles in each cell type. Kim et al. exposed NHBE and A549 cells to SiO_2-NPs in order to determine cytotoxicity, method of cell death, and intracellular NP accumulation [76]. NHBE and A549 cells were exposed to 10-400 μg/mL of SiO_2-NPs for 4 hours. Cell viability was seen to decrease significantly at 100 μg/mL for both cell lines. SiO_2-NPs were found to induce necrosis in NHBE and A549 as well. Flow cytometry was used to measure the retention of FITC-labeled SiO_2-NPs. The authors found that SiO_2-NPs were contained in 95.62% of NHBE cells and 99.47% of A549 cells after exposure. In another study by Frontiñan-Rubio et al., the authors used NHBE and A549 cells to assess the toxic effects of GONPs [77]. NHBE exposure to 5 μg/mL of GONPs for 6 hours was seen to significantly increase necrosis and apoptosis. Comparatively, A549 exposure to 5 μg/mL of GONPs for 24 hours was seen to increase necrotic and apoptotic cells to a lesser degree. They found a slight, nonsignificant decrease in cell viability for 24-hour exposure to 5 μg/mL of GONPs, while A549 cells remained unchanged. Oxidative stress was also examined by measuring hydrogen peroxide (H_2O_2) and superoxide anion (O_2^-) levels. There was a 51.3% increase in H_2O_2 for NHBE exposed to 5 μg/mL of GONPs for 24 hours. However, O_2^- levels remained the same after NHBE exposure to GONPs. No changes in H_2O_2 or O_2^- levels were observed in A549 cells. These results show that A549 cells are more resistant to GONPs than the NHBE. On another note, Hussain et al. exposed NHBE and 16HBE cell lines to 20 μg/cm² of TiO_2-NPs for 4 hours [78]. They revealed that TiO_2-NPs caused intracellular ROS production in both NHBE and 16HBE cells after 30 minutes of exposure. DNA fragmentation was also seen in the cells, which confirms the occurrence of apoptosis. They found that TiO_2-NPs induce apoptosis by destabilizing lysosomal membranes. Specifically, the proteases released by the damaged membrane have a significant role in apoptosis. Destabilization of the lysosomal membrane was observed after 30 minutes of exposure to TiO_2-NPs. These findings are corroborated by Smallcombe et al., in which the authors exposed NHBE and 16HBE to 10–100 μg/mL of TiO_2-NPs [40]. They showed that TiO_2-NPs caused barrier disruption and AJC disassembly. For 16HBE, there was a significant decrease in TEER for 25-100 μg/mL of TiO_2-NPs. Likewise, NHBE exposure to 25-100 μg/mL of TiO_2-NPs induced a significant decrease in TEER. This indicates that exposure to TiO_2-NPs increases the permeability of cell monolayers, which is in accordance with past studies on AEC exposure to TiO_2-NPs.

 doi:10.20944/preprints202406.1674.v1

Immunolabeling of TJ and AJ proteins demonstrated that exposure to TiO_2-NPs damaged the normal "chicken wire" strands seen in the control cells. They observed more gaps and decreased labeling intensity in monolayers exposed to TiO_2-NPs. Furthermore, this study examined the effects of TiO_2-NPs on RSV-infected 16HBE cells. In the presence of RSV, TiO_2-NPs amplified RSV infection and its damaging effects on the AJC. This reflects the role of nanoparticles in exacerbating the harmful effects of preexisting pulmonary conditions.

The impact of nanoparticles on primary and immortalized cell lines is generally concurring. However, differences in pro-inflammatory responses between NHBE and immortalized epithelial cells have also been published. Notably, a study by Ekstrand-Hammarström et al. compared cellular responses of NHBE and A549 cells that were exposed to TiO_2-NPs and found that both cell lines showed similar changes in cell viability and oxidative stress, while cytokine production differed [79]. The investigators used five different TiO_2-NPs, characterized by size and photocatalytic activity (anatase or rutile): 9 nm rutile (R9), 5 nm rutile (R5), 14 nm anatase (A14), 60 nm anatase (A60), and 20 nm mixed anatase and rutile (P25). First, both cell lines were exposed to 5-200 μg/mL of TiO_2-NPs for 24 hours and ROS production was measured at 2- and 24-hour time points. They showed that P25 and rutile TiO_2-NPs caused significant ROS production in NHBE and A549 at both 2 and 24 hours. To measure cell viability, NHBE and A549 were exposed to 0.19-400 μg/mL of TiO_2-NPs for 24 hours. There was a nonsignificant decrease in cell viability for both NHBE and A549 at 400 μg/mL. Following this, they evaluated the pro-inflammatory responses of the cell lines by measuring cytokine secretion. NHBE and A549 were exposed to 10, 50, and 250 μg/mL of TiO_2-NPs for 24 hours. There was a significant increase in IL-8, a pro-inflammatory cytokine, secretion at 50 μg/mL of P25 for both NHBE and A549. Moreover, at exposure to 100 μg/mL of P25, there was a strong expression of cytokines IL-1β, VEGF, and G-SCF for NHBE cells that were not seen in the A549. This clarifies that nanoparticle-induced cytokine release varies with the cell culture model and composition of nanoparticles that are used.

Similarly, a study by Schlinkert et al. compared NHBE and A549 cells by exposing them to 0.1-0.8 μg/cm² of AgNPs and AuNPs for 24 hours [80]. There was no significant cytotoxicity observed in A549 cells. On the other hand, 0.4 and 0.8 μg/cm² of AgNPs caused a significant increase in LDH release for NHBE, showing cytotoxicity in higher nanoparticle concentrations. Cell viability was seen to decrease substantially in NHBE exposed to 0.7-0.8 μg/cm² of AgNPs and AuNPs, while no changes were seen in A549 cells. Remarkably, ROS production was seen to be the most minimal in NHBE compared to the A549. This result contradicts Frontiñan-Rubio et al.'s findings that NHBE cells are more sensitive to GONPs than A549 cells in terms of oxidative stress. However, considering the difference in properties of GONPs and AgNPs, it is evident that the cellular responses and susceptibility of each cell line depend on the type of nanoparticle to which it is exposed.

3. Animal Models of Nanoparticle Toxicity on the Airway:

Animal models are useful in assessing the impact of nanoparticle toxicity on the airway barrier because of their ability to manipulate the environment in a way that mimics real-life conditions. Specifically, many mouse and rat studies have looked at the effect of nanoparticles via inhalation on lung inflammation and other physiological responses [81–83] (**Table 2**). Moreover, animal models with pre-existing conditions are frequently used to study the impact of nanoparticle toxicity on the respiratory tract. This is beneficial because nanoparticle retention and clearance may show to be different in the presence of chronic diseases. Using murine models can shed light on the mechanism by which nanoparticles disrupt lung function, cause inflammation, and aggravate underlying pulmonary diseases.

Table 2. Effects of nanoparticle exposure on murine models.

Nanoparticle Type	Murine Model	Concentration & Exposure Route	Inflammatory Response	BALF Analysis and Other Cellular Responses	Reference

 doi:10.20944/preprints202406.1674.v1

	Male C57BL/6J mice	1 mg/mL, Oropharyngeal aspiration	↑ Expression of MIP-2, MCP-1, IL-6, IL-1β, CXCL1	↑ Total cell count ↑ Neutrophil count	[84]
AgNPs	Male F344/DuCrl rats	41-1105 μg/m³, Nose-only inhalation	↑ Expression of MCP-1, IL-1β	↑ Total cell count ↑ Neutrophil count ↑ LDH release ↑ Concentration-dependent lung deposition	[85]
ZnO-NPs	Male F344 rats	0.8 and 4 mg/kg, Intratracheal instillation	↑ CINC-1 and CINC-2	↑ Total cell count ↑ Neutrophil count ↑ LDH release ↑ Oxidative stress ↑ Macrophage count	[86]
		2 and 10 mg/m³, Inhalation*	*(Only seen at highest concentration)*	*(Only seen at highest concentration)*	
	Male C57BL/6 mice	3.5 mg/m³, Inhalation, 2 weeks	↑ Expression of IL-12p(40) and MIP-1α	↑ Zn^{2+} ions ↑ Total cell count ↑ Neutrophil count ↑ Macrophage count ↑ LDH release ↑ Hematocrit	[87]
		3.5 mg/m³, Inhalation, 13 weeks	-	↑ Zn^{2+} ions ↑ Total cell count ↑ Macrophage count ↑ Hematocrit	
	Male Wistar rats	100 mg/kg, Oral gavage	↑ TNF-α and IL-6 levels	↑ 8-OHdG levels ↓ Glutathione (GSH)	[96]
	Female BALB/cJ mice	4-271 mg/m³, Inhalation	-	↑ Neutrophil count ↑ Lymphocyte count ↑ Break time	[97]
	Female C57BL/6 mice		↑ Leukocyte count	↑ Total protein	[40]

 doi:10.20944/preprints202406.1674.v1

TiO_2-NPs		0.5-5 mg/kg, Intranasal instillation	↑ Expression of IL-1α, IL-6, IL-10, TNFα, IFNγ, MCP-1, RANTES, LIF, IP-10	↑ Barrier permeability	
	Female BALB/c/Sca mice	10 ± 2 mg/m³, Inhalation, Asthmatic mice	↓ Expression of IL-1β, TNF-α, IL-4, IL-13, IL-10, Foxp3 ↓ Expression of CCL-3, CXCL5, CXCL2 ↓ IgE levels	↓ Eosinophil count ↓ Lymphocyte count ↓ PAS+ goblet cells	[82]
		10 ± 2 mg/m³, Inhalation, Healthy mice	↓ Expression of IL-1β ↑ Expression of CXCL5	↑ Neutrophil count	
	Male C57BL/6 mice	0.77-7.03 mg/m³, Inhalation	↑ Expression of IL-1β and IL-6	↑ Total cell count ↑ Macrophage count	[88]
		0.1-3.0 mg/mL, Intranasal instillation		↑ Total cell count ↑ Neutrophil count	
	Female BALB/cJ mice	4-271 mg/m³, Inhalation	-	↑ DNA damage ↑ Break time	[97]
CeO_2-NPs	Male CD1 mice	2 mg/m³, Inhalation	↑ Expression of TNF-α, IL-1β, and IL-6	↓ Cell viability ↑ Neutrophil count ↑ Total protein ↓ Glutathione (GSH)	[90]
	Male and female BALB/c mice	0.1 or 0.5 mg/kg, Intratracheal instillation	↑ Expression of TNF-α ↓ Catalase	↑ Total cell count ↑ Neutrophil count	[91]
	Male and female Wistar rats	641 mg/m³, Inhalation	↑ Leukocyte count ↑ Expression of TNF-α, IL-1β, and IL-6	↓ Cell viability ↑ Total cell count ↑ LDH release	[92]

 doi:10.20944/preprints202406.1674.v1

				↑ Neutrophil count	
	Male Sprague-Dawley rats	2.7 mg/m^3, Inhalation	-	↑ LDH release ↑ PMNs	[93]
	Female BALB/cJ mice	4-271 mg/m^3, Inhalation	-	↑ Neutrophil count ↑ Lymphocyte count	[97]
Al_2O_3-NPs	Male Sprague-Dawley rats	0.2, 1, and 5 mg/m^3, Nasal inhalation	↑ Expression of TNF-α and IL-6	↑ Total cell count ↑ LDH release	[95]
	Male Wistar rats	70 mg/kg, Oral gavage	↑ TNF-α and IL-6 levels	↑ 8-OHdG levels ↓ Glutathione (GSH)	[96]
CoNPs	Male and female gpt delta transgenic mice	50 µg, Intratracheal instillation	↑ CXCL1/KC levels	↑ LDH release ↑ Neutrophil count ↑ Macrophage count ↑ Total protein ↑ DNA damage	[98]
	Sprague-Dawley rats	100 mg, Bilateral implantation	-	↑ Nuclei and mitotic rates ↑ Expression of PCNA	[99]
CoO-NPs	Female rats	40, 100, and 400 µg/rat, Intratracheal instillation	↑ IL-6, eotaxin, and IL-13 levels ↑ Eosinophilic inflammation	↑ LDH release ↑ Total protein ↑ Solubility in ALF	[100]
Co_3O_4-NPs			↑ CINC-3 levels ↑ Neutrophilic inflammation	↑ LDH release *(Only seen at highest concentration)* ↓ Solubility in ALF	
	C57BL/6 mice	2.5, 5, 10 mg/kg, Intranasal instillation	↑ Expression of CCL-2, IL-4, TNF-α, α-SMA and collagen-I	↑ Apoptosis	[101]
CuO-NPs	Female C57BL/6 mice	15 µg/bolus, Intranasal instillation	↑ Leukocyte count ↑ HMGB1, IL-1β, and TNF-α levels	↑ Neutrophil count ↑ Protein chlorination ↑ Total protein	[102]

 doi:10.20944/preprints202406.1674.v1

Male Sprague-Dawley rats	0.15 and 1.5 mg/kg, Intratracheal instillation	↑ MIP-2 and TNF-α levels	↑ Total cell count ↑ PMN count ↑ Total protein ↑ LDH release ↓ Expression of catalase, Gpx-1, and Prx-2	[103]

List of abbreviations: 8-OHdG, 8-hydroxy-2′-deoxyguanosine; α-SMA, alpha-smooth muscle actin; AgNPs, silver nanoparticles; ALF, artificial lysosomal fluid; Al_2O_3-NPs, aluminum oxide nanoparticles; BALF, bronchoalveolar lavage fluid; CCL-2, chemokine (C-C motif) ligand 2; CCL-3, macrophage inflammatory protein 1-α; CeO_2-NPs, cerium oxide nanoparticles; CINC-1, -2, -3, cytokine-induced neutrophil chemoattractant 1, 2, 3; CoNPs, cobalt nanoparticles; CoO-NPs, cobalt (II) oxide nanoparticles; Co_3O_4-NPs, cobalt (II, III) oxide nanoparticles; CuO-NPs, copper oxide nanoparticles; CXCL1, growth-regulated oncogene alpha; CXCL2, macrophage inflammatory protein-2; CXCL5, CXC chemokine ligand 5; Foxp3, forkhead box P3; GSH, glutathione; Gpx-1, glutathione peroxidase-1; HMGB1, high mobility group box 1; IFNγ, interferon gamma; IgE, immunoglobulin E; IL-1α, -1β, -4, -6, -10, and -13, interleukin-1, alpha, beta, 4, 6, 10, and 13; IL-1β, interleukin-1 beta; IL-12p(40), interleukin-12 subunit p40; IP-10, interferon-gamma inducible protein of 10 kDa; LDH, lactate dehydrogenase; LIF, leukemia inhibitory factor; MCP-1, monocyte chemoattractant protein-1; MIP-1α and -2, macrophage inflammatory protein-1 alpha and 2; PAS, periodic acid-Schiff; PCNA, proliferating cell nuclear antigen; PMNs, polymorphonuclear neutrophils; Prx-2, peroxiredoxin-2; RANTES, regulated upon activation, normal T cell expressed, and secreted; TiO_2-NPs, titanium dioxide nanoparticles; TNF-α, tumor necrosis factor alpha; ZnO-NPs, zinc oxide nanoparticles; ↓, decreased; ↑, increased; -, not determined.

3.1. Silver Nanoparticles (AgNPs)

A study by Alqahtani et al. examined the impact of AgNPs on mice exhibiting metabolic syndrome (MetS), which include conditions like high cholesterol, hypertension, and insulin resistance [84]. Male C57BL/6J mice were fed either a regular diet or a high-fat Western diet (HFWD) to increase cholesterol and body weight for 14 weeks. The mice were exposed to 1 mg/mL of AgNPs via oropharyngeal aspiration, and acute toxicity was measured 24 hours after exposure. The authors found that AgNP exposure significantly increased mRNA expression of pro-inflammatory mediators MIP-2, MCP-1, IL-6, IL-1β, and CXCL1 in both control and MetS mice. MetS mice exhibited even higher enhanced levels of MIP-2, IL-6, and MCP-1 compared to the healthy mice. Additionally, bronchoalveolar lavage fluid (BALF) analysis demonstrated that total cell and neutrophil counts were higher in both control and MetS mice exposed to AgNPs. Together, these responses provide evidence that AgNPs induce lung inflammation and the presence of MetS exacerbates this effect. In another study, Braakhuis et al. exposed male F344/DuCrl rats to AgNPs ranging from 41 to 1105 mg/m^3 of air for 4 days [85]. They analyzed BALF and found a concentration-dependent increase in the number of cells, neutrophils, and pro-inflammatory markers IL-1β and MCP-1. The authors observed an increase in the total lung deposition of nanoparticles as the concentration of AgNP-exposure increased. The total amount of AgNPs in the lungs decreased for all concentrations 7 days after the initial exposure. The findings of the study indicate how AgNPs lead to pulmonary toxicity and inflammation.

3.2. Zinc Oxide Nanoparticles (ZnO-NPs)

Similarly, animal studies show that ZnO-NPs cause inflammatory responses in the lung, although at lower toxicity levels than AgNPs. For example, Morimoto et al. exposed male F344 rats to 0.8 mg/kg and 4 mg/kg of ZnO-NPs by intratracheal instillation as well as 2 and 10 mg/m^3 of ZnO-NPs via inhalation for 6 hours every day [86]. In the BALF of rats exposed to ZnO-NPs via intratracheal instillation, there was a significant increase in the total cell and neutrophil count for all concentrations. On the other hand, rats that were exposed to ZnO-NPs via inhalation showed the

 doi:10.20944/preprints202406.1674.v1

same results only at the highest concentration. Furthermore, expression of HO-1, an enzyme that is produced in response to oxidative stress, followed the same trend. Rats exposed to ZnO-NPs by intratracheal instillation had significantly higher HO-1 levels at all ZnO-NP concentrations, while this only held true at 10 mg/m^3 of ZnO-NPs for rats that were exposed via inhalation. It is important to mention that these findings were not persistent. BALF was analyzed at different time points ranging from 3 days to 6 months following the completion of instillation or inhalation exposure. Significant results were only seen at the 3-day mark, which shows that the toxic effects of ZnO-NPs are somewhat transient. To corroborate, Adamcakova-Dodd et al. examined the toxic effects in mice after sub-acute or sub-chronic exposure to ZnO-NPs [87]. They exposed male C57BL/6 mice to 3.5 mg/m^3 of ZnO-NPs for 4 hours a day for a duration of 2 or 13 weeks to mimic sub-acute and sub-chronic conditions, respectively. There was an increased amount of Zn^{2+} ions in the BALF right after exposure to ZnO-NPs, but this reverted back to baseline concentrations after 3 weeks following exposure. In the mice exposed for 2 weeks, the authors found a significant increase in macrophages and a nonsignificant increase in IL-12(p40) and MIP-1α, which are inflammatory cytokines. However, the parameters for measuring lung toxicity did not differ significantly for the sub-chronic mice. Like Morimoto et al., this study reveals the relatively low toxicity of ZnO-NPs in murine models, especially for long-term inhalation exposure.

3.3. Titanium Dioxide Nanoparticles (TiO_2-NPs)

Evidence has shown that TiO_2-NPs have different effects on murine models based on the type of disease present in the animal. Smallcombe et al. exposed female C57BL/6 mice to RSV and approximately 0.5-5 mg/kg of TiO_2-NPs via intranasal instillation [40]. They collected BALF 4 days after RSV infection. Leukocyte count was significantly greater at concentrations of 2 and 3 mg/kg of TiO_2-NPs, indicating inflammation of the airway barrier. Total BALF protein levels were elevated for all concentrations as well, showing increased permeability and characteristic of a disrupted airway barrier. In addition, hematoxylin and eosin (H&E) staining of lung tissue demonstrated thickening of the airway wall and increased immune cells. This result further confirms the dose-dependent inflammation response induced by TiO_2-NPs and RSV, both separately and together. Intriguingly, TiO_2-NPs have been found to reduce pulmonary inflammation in asthmatic mice. Rossi et al. exposed female BALB/c/Sca mice to 10 ± 2 mg/m^3 of TiO_2-NPs three times a week for a total of four weeks [82]. The mice in the asthmatic condition were given 20 μg of ovalbumin intraperitoneally. The authors observed that healthy mice showed a significant increase in CXCL5, a chemokine that modulates leukocyte activity. However, asthmatic mice showed decreased levels of pro-inflammatory cytokines and chemokines. This points to how nanoparticles can suppress, rather than antagonize, the immune responses of certain respiratory conditions. Different-sized nanoparticles can also elicit varying inflammatory responses. In a study by Grassian et al., male C57BL/6 mice were exposed to TiO_2-NPs ranging from 5 to 21 nm in size through either a whole-body exposure chamber or nasal instillation for 4 hours and necropsied immediately or 24 hours after the exposure [88]. BALF was utilized to quantify the total protein amount, LDH activity, and concentrations of cytokines IL-1β, IL-6, and TNF-α. The researchers discovered that the larger 21 nm TiO_2-NPs induced greater inflammatory responses compared to the 5 nm TiO_2-NPs. The BALF of mice exposed to the 21 nm TiO_2-NPs exhibited a significantly increased number of neutrophils and LDH activity, which were not observed in those exposed to the 5 nm TiO_2-NPs. Additionally, the larger TiO_2-NPs prompted elevated concentrations of IL-1β and IL-6, while no change in TNF-α levels was noted. The authors concluded that the TiO_2-NPs were delivered to the mice as agglomerates rather than individual particles, suggesting that the packing of nanoparticles could decrease the total surface area that is exposed to the mice, thus reducing nanoparticles toxicity. Therefore, the agglomeration state is an important factor when assessing nanoparticle toxicity *in vivo*.

3.4. Cerium Oxide Nanoparticles (CeO_2-NPs)

Previous studies have demonstrated that CeO_2-NPs induce inflammation and oxidative stress in mouse and rat models. CeO_2-NPs, commonly used as a diesel fuel additive, can lead to intracellular

 doi:10.20944/preprints202406.1674.v1

ROS production due to their oxidizing abilities [89]. Aalapati et al. exposed male CD1 mice to 2 mg/m^3 of CeO_2-NPs via inhalation for 6 hours per day for 0, 7, 14, and 28 days [90]. BALF collected 1 day after exposure and was analyzed for inflammatory responses. The study revealed a time-dependent decrease in cell viability over the 28-day exposure period. Neutrophil count in BALF was significantly higher in mice exposed to CeO_2-NPs, an indication of pulmonary inflammation. Furthermore, pro-inflammatory cytokines TNF-α, IL-1β, and IL-6 significantly increased, also in a time-dependent manner. Increased protein levels in BALF of mice exposed for 28 days indicated decreased integrity of the airway epithelial barrier. A significant decrease in glutathione (GSH) levels in mice exposed to CeO_2-NPs supported the occurrence of oxidative stress in epithelial cells. Histological analysis showed damage to the airway barrier, manifested as necrosis, fibrosis, proteinosis, and apparent granulomas in the pulmonary parenchyma. Similarly, Nemmar et al. investigated the impact of acute exposure to CeO_2-NPs on the lungs [91]. Male and female BALB/c mice were exposed to 0.1 or 0.5 mg/kg of CeO_2-NPs via intratracheal instillation. BALF collected 24 hours after initial delivery of CeO_2-NPs showed significantly elevated total cell and neutrophil counts at both concentrations. CeO_2-NPs induced an increase in TNFα, an inflammatory cytokine, and a decrease in catalase activity, an antioxidant enzyme, in BALF of exposed mice. Correspondingly, lung sections from mice showed that exposure to CeO_2-NPs led to a dose-dependent increase in neutrophils and macrophages in the alveolar interstitial space. This study further demonstrates the oxidative stress and inflammation of the lungs caused by CeO_2-NPs. Rat models have shown similar outcomes. Srinivas et al. examined the toxic effects of CeO_2-NPs on male and female Wistar rats [92]. Rats were exposed to approximately 641 mg/m^3 of CeO_2-NPs via inhalation for 4 hours, and BALF was collected at 24 hours, 48 hours, and 14 days following the exposure. The authors observed a significant decrease in cell viability and an increase in total cell count at all time points. BALF analysis revealed significant increases in lactate dehydrogenase, total leukocyte count, and neutrophils. Rats exposed to CeO_2-NPs showed an increase in pro-inflammatory cytokines IL-1β, TNF-α, and IL-6 in both BALF and blood samples, indicating initiation of inflammatory responses. The presence of microgranulomas in the pulmonary parenchyma at the 14-day mark suggested a dysfunctional clearance mechanism resulting in CeO_2-NP persistence in the lungs. Likewise, Demokritou et al. exposed male Sprague-Dawley rats to 2.7 mg/m^3 of CeO_2-NPs or CeO_2-NPs coated in SiO_2 for 2 hours a day over 4 days via a whole-body inhalation chamber [93]. They found a significant increase in polymorphonuclear neutrophils (PMNs) and lactate dehydrogenase (LDH), markers for inflammation and cytotoxicity, respectively. BALF analysis of mice exposed to SiO_2-coated CeO_2-NPs showed similar levels of albumin, PMNs, and LDH to those of healthy mice, indicating that encapsulation in SiO_2 attenuated the adverse effects of CeO_2-NPs. The authors highlighted the harmless nature of amorphous SiO_2 as a reason why cells did not exhibit toxicity when exposed to CeO_2-NPs coated by SiO_2.

3.5. Aluminum Oxide Nanoparticles (Al_2O_3-NPs)

Past research has indicated that Al_2O_3-NPs are less toxic than other metal oxide nanoparticles [94]. However, murine studies suggest potential inflammatory effects of Al_2O_3-NPs on the respiratory system. In a study by Kim et al., male Sprague-Dawley rats were exposed to 0.2, 1, and 5 mg/m^3 of Al_2O_3-NPs for 28 days via nasal inhalation only [95]. BALF analysis showed a significantly higher count of total cells and neutrophils in the rats exposed to Al_2O_3-NPs at 1 and 5 mg/m^3 of Al_2O_3-NPs. Lactate dehydrogenase, TNF-α, and IL-6 levels were also elevated at these concentrations. Examination of lung sections revealed alveolar macrophage accumulation in half of the mice exposed to 5 mg/m^3 of Al_2O_3-NPs. Consistently, Yousef et al. compared the toxic impacts of Al_2O_3-NPs and ZnO-NPs [96]. Male Wistar rats were exposed to 70 mg/kg of Al_2O_3-NPs, 100 mg/kg of ZnO-NPs, or a combination of both daily via oral gavage for 75 days. They found that exposure to Al_2O_3-NPs and ZnO-NPs separately caused an increase in 8-hydroxy-2′-deoxyguanosine (8-OHdG), a biomarker for measuring oxidative damage to DNA, as well as cytokines TNF-α and IL-6. These results were accompanied by a decrease in GSH levels, indicating that both Al_2O_3-NPs and ZnO-NPs induced oxidative stress in lung tissues. The combination of Al_2O_3-NPs and ZnO-NPs exacerbated these results to a small degree.

 doi:10.20944/preprints202406.1674.v1

A comparison study of ZnO-NPs, TiO_2-NPs, Al_2O_3-NPs, and CeO_2-NPs was conducted by Larsen et al. to examine the acute and persistent impacts of each nanoparticle type [97]. Female BALB/cJ mice were exposed to an average of 4 to 271 mg/m^3 of ZnO-NPs, TiO_2-NPs, Al_2O_3-NPs, and CeO_2-NPs via inhalation for 60 minutes. Lung inflammation was observed in BALF of mice exposed to ZnO-NPs 24 hours post-exposure, as there was a significant increase in neutrophils and lymphocytes. However, this increase was not observed in TiO_2-NPs or Al_2O_3-NPs. Mice exposed to CeO_2-NPs showed elevated neutrophil and lymphocyte levels at 13 weeks post-exposure. Interestingly, only TiO_2-NPs showed a significant increase in DNA-strand breaks, indicating damage to DNA. The amount of break time taken during the inhalation period by each mouse was used to determine their nose irritation response. A significantly higher break time was observed in mice exposed to TiO_2-NPs and ZnO-NPs but not for Al_2O_3-NPs or CeO_2-NPs. The authors found that ZnO-NPs induced more intense and persistent damaging effects than the other nanoparticles. Overall, TiO_2-NPs and Al_2O_3-NPs were ranked as having low inflammatory responses and potency, while CeO_2-NPs fell in between ZnO-NPs and TiO_2-NPs/Al_2O_3-NPs.

3.6. Cobalt Nanoparticles (CoNPs)

Like other transition metal nanoparticles, CoNPs and CuO-NPs have been shown to induce oxidative stress, inflammation, and DNA damage. For instance, Wan et al. exposed male and female *gpt* delta transgenic mice to 50 μg of CoNPs via intratracheal instillation [98]. BALF was collected at time points 1, 3, 7, and 28 days, or four months after the initial delivery of CoNPs. The authors observed an increase in neutrophils, LDH activity, total protein levels, and the amount of chemokine CXCL1/KC in the BALF of mice exposed to CoNPs. Histopathological analysis showed that neutrophils and macrophages infiltrated the alveolar space and interstitial tissues 7 days after instillation of CoNPs. The alveolar wall was also thickened. These findings indicate lung injury and inflammation. Immunohistochemical staining of Ki-67 and PCNA, indicators of cell proliferation, and γ-H2AX, which measures DNA damage, was performed. Ki-67 and PCNA were confirmed to be in the nucleus, and the number of Ki-67- and PCNA-positive cells significantly increased. Even at the 4-month mark, CoNPs were found to elevate Ki-67 and PCNA levels. Furthermore, CoNPs induced DNA damage, shown by the higher frequency of transversion mutations and 8-OHdG levels in lung tissue. In another study, Hansen et al. investigated the effect of CoNPs on the formation of sarcomas using a rat model [99]. They bilaterally implanted 100 mg of CoNPs in Sprague–Dawley rats for 6, 8, or 12 months. At the 6-month time point, histological analysis found the presence of preneoplasia in 3 of the rats exposed to CoNPs. The authors observed enhanced nuclei and mitotic rates, as well as expression of PCNA in mesenchymal cells of these rats. The findings for rats implanted with CoNPs show that initial inflammation led to preneoplasia, which eventually presents as neoplasia. This sequence is consistent with the pathogenesis of malignant tumors. Therefore, the findings of this study establish the role of CoNPs in advancing the process of neoplasia. It is worth noting that different Co-based nanoparticles elicit distinct responses. To highlight, Jeong et al. compared the effects of CoO-NPs and Co_3O_4-NPs on female rats [100]. The rats were exposed to 40, 100, and 400 μg/rat of CoO-NPs and Co_3O_4-NPs via intratracheal instillation. BALF collected 24 hours after instillation showed that LDH levels followed a dose-dependent significant increase for rats exposed to CoO-NPs. However, Co_3O_4-NPs only induced a significant elevation in LDH only at the highest dose, 400 μg/rat. Total protein concentration was significantly higher at 100, and 400 μg/rat of CoO-NPs, while rats exposed to Co_3O_4-NPs did not show any significant increases. The authors observed that Co_3O_4-NPs only induced an increase in cytokine-induced neutrophil chemoattractant-3 (CINC-3) levels. On the other hand, exposure to CoO-NPs led to greater levels of other pro-inflammatory cytokines such as IL-6, eotaxin, and IL-13. Additionally, two different types of inflammatory responses were shown. Rats instilled with CoO-NPs produced eosinophilic inflammation, while Co_3O_4-NPs led to neutrophilic inflammation. The contrast in cellular responses can be explained by the solubility properties of CoO-NPs and Co_3O_4-NPs. The investigators measured the solubility percentage of each nanoparticle type in artificial lysosomal fluid (ALF). They found that CoO-NPs had 92.65% solubility and Co_3O_4-NPs had 11.46% solubility in ALF. Thus, the reported results

 doi:10.20944/preprints202406.1674.v1

support how varying physicochemical characteristics within the same element can enhance its inflammation and toxicity levels.

3.7. Copper Oxide Nanoparticles (CuO-NPs)

Similarly, Lai et al. investigated the impact of CuO-NPs on C57BL/6 mice [101]. They exposed the mice to 2.5 mg/kg, 5 mg/kg, and 10 mg/kg of CuO-NPs via intranasal instillation, and inflammation parameters were assessed at 7, 14, and 28 days after the initial exposure. Hematoxylin & Eosin (H&E) staining of lung tissue collected at the 14-day mark showed inflammation. This was supported by a significant increase in pro-inflammatory gene expression such as CCL-2, IL-4, and TNF-α for 5 mg/kg of CuO-NPs. The authors also observed expression of α-SMA, a marker for myofibroblast activation, and collagen-I in mice exposed to CuO-NPs, indicating that CuO-NPs induce lung fibrosis in addition to inflammation. Likewise, Pietrofesa et al. exposed female C57BL/6 mice to 15 μg/bolus of CuO-NPs via intranasal instillation, and BALF was collected at 1, 3, and 7 days after instillation [102]. At the 1-day time point, a significant increase in leukocyte, total protein, and neutrophil count was observed in BALF of mice exposed to CuO-NPs. The authors found a significant elevation in protein chlorination, caused by the influx of neutrophils and macrophages abundant in myeloperoxidase (MPO), which release HOCl when inflammation occurs. Proinflammatory cytokine levels of HMGB1, IL-1β, and TNF-α were significantly increased as well. These data show how CuO-NPs lead to pulmonary injury and inflammation in the murine lung. Additionally, Kwon et al. intratracheally instilled 0.15 and 1.5 mg/kg of CuO-NPs to male Sprague–Dawley rats [103]. Analysis of BALF taken 24 hours after the exposure showed a significant increase in the total cell and polymorphonuclear leukocyte (PMN) count in a dose-dependent manner. LDH activity and protein concentration in the BALF were also elevated compared to the healthy rats. Cytokine levels of MIP-2 and TNF-α were increased significantly in rats exposed to 1.5 mg/kg of CuO-NPs. Lung sections of rats exposed to CuO-NPs exhibited acute inflammation in the bronchioles and alveoli region. The highest concentration of CuO-NPs induced pulmonary edema in the lung tissue. Lastly, antioxidant expression of catalase, Gpx-1, and Prx-2 was downregulated in the rats exposed to 1.5 mg/kg of CuO-NPs.

4. Conclusion and Future Direction

Nanoparticles, categorized as metal, metal oxide, or non-metal, are extensively employed owing to their unique properties. However, exposure to nanoparticles via inhalation can cause detrimental effects on the respiratory tract. The airway epithelial barrier is a vital part of the human body's innate immune system. TJs and AJs make up the AJC, which provide a barrier to inhaled pathogens and environmental particulate matter [104]. Markedly, the AJC facilitates the interactions between nanoparticles and the airway barrier. Previous research has shown that nanoparticles, especially those containing metal groups, disrupt the airway epithelial barrier and lead to increased barrier permeability, apoptosis, ROS production, DNA damage, and inflammation.

While there is expanding knowledge on the impact of different nanoparticle types on the airway epithelial barrier, there are limitations to current studies. Establishing a controlled environment that resembles real-world human exposure conditions is crucial but challenging for in vivo and in vitro experiments. To address this, utilizing combined exposure methods to multiple nanoparticle types or environmental pollutants will be more representative of the human surroundings. Also, extending the exposure time to look at the long-term effects of nanoparticles on the airway barrier can be beneficial for studying chronic respiratory outcomes. This prolonged exposure allows for greater insight into the progression of underlying pulmonary conditions and possible cumulative effects of pollutants. In addition, incorporating a wide range of nanoparticle concentrations can inform us of the dose-dependent relationship between nanoparticles and physiological responses. Furthermore, when comparing data from cell culture and murine studies, it is necessary to use standardized methods to ensure reliability of the results.

Recent cell culture and murine model studies have focused on the cellular responses to different metal and non-metal nanoparticles. Specifically, these investigations looked at airway epithelial

 doi:10.20944/preprints202406.1674.v1

barrier disruption, inflammatory reactions, and oxidative stress. The variation in nanoparticle composition plays a pivotal role in determining its impact on the respiratory tract. Understanding the specific effects of nanoparticle types on the airway epithelial barrier may advance the development of tailored experimental models and potential therapeutic interventions for nanoparticle-induced barrier disruption.

Author Contributions: Conceptualization, C.L. and F.R.; Writing – Original Draft Preparation, C.L. and F.R.; Writing – Review & Editing, C.L. and F.R.; Visualization, C.L. and F.R.; Supervision, F.R.; Funding Acquisition, F.R.

Funding: This work was supported by the National Institutes of Health (R01HL148057 to F.R.).

Data Availability Statement:

Conflicts of Interest: The authors report there are no competing interests to declare.

Abbreviations:

16HBE – 16HBE14o- human bronchial epithelial
A549 – human A549 adenocarcinoma
AEC – airway epithelial cell
AgNPs – silver nanoparticles
AJ – adherens junction
AJC – apical junctional complex
Al_2O_3-NPs – aluminum oxide nanoparticles
AuNPs – gold nanoparticles
Calu-3 – cultured human airway epithelial
cAMP – cyclic adenosine monophosphate
$CaSO_4$-NPs – calcium sulfate nanoparticles
CeO_2-NPs – cerium oxide nanoparticles
CoNPs – cobalt nanoparticles
CuO-NPs – copper oxide nanoparticles
GONPs – graphene oxide nanoparticles
LDH – lactate dehydrogenase
NHBE – normal human bronchial epithelial
$PbSO_4$-NPs – lead sulfate nanoparticles
ROS – reactive oxygen species
SiO_2-NPs – silicon dioxide nanoparticles
TEER – transepithelial electrical resistance
TiO_2-NPs – titanium dioxide nanoparticles
TJ – tight junction
ZO – zonula occludens
ZnO-NPs – zinc oxide nanoparticles
$ZnSO_4$-NPs – zinc sulfate nanoparticles

References

1. Altammar, K.A., A review on nanoparticles: characteristics, synthesis, applications, and challenges. Front Microbiol, 2023. **14**: p. 1155622.
2. Rizvi, S.A.A. and A.M. Saleh, *Applications of nanoparticle systems in drug delivery technology.* Saudi Pharm J, 2018. **26**(1): p. 64-70.
3. Helal, M., et al., Evaluating the coating process of titanium dioxide nanoparticles and sodium tripolyphosphate on cucumbers under chilling condition to extend the shelf-life. Sci Rep, 2021. **11**(1): p. 20312.
4. Rokayya, S., et al., Application of nano-titanum dioxide coating on fresh Highbush blueberries shelf life stored under ambient temperature. LWT, 2021. **137**: p. 110422.
5. Li, Q., et al., Impact of food additive titanium dioxide on the polyphenol content and antioxidant activity of the apple juice. LWT, 2022. **154**: p. 112574.

 doi:10.20944/preprints202406.1674.v1

6. Ibrahim, K., S. Khalid, and K. Idrees, *Nanoparticles: Properties, applications and toxicities.* Arabian Journal of Chemistry, 2019. **12**(7): p. 908-931.
7. Pujalté, I., et al., Characterization of Aerosols of Titanium Dioxide Nanoparticles Following Three Generation Methods Using an Optimized Aerosolization System Designed for Experimental Inhalation Studies. Toxics, 2017. **5**(3).
8. Rajasekar, M., et al., Recent developments in sunscreens based on chromophore compounds and nanoparticles. RSC Adv, 2024. **14**(4): p. 2529-2563.
9. Joudeh, N. and D. Linke, Nanoparticle classification, physicochemical properties, characterization, and applications: a comprehensive review for biologists. Journal of Nanobiotechnology, 2022. **20**(1): p. 262.
10. Chetan, P., et al., *Biological agents for synthesis of nanoparticles and their applications.* Journal of King Saud University - Science, 2022. **34**(3): p. 101869.
11. Moreno Ruiz, Y.P., et al., Advanced Hydrogels Combined with Silver and Gold Nanoparticles against Antimicrobial Resistance. Antibiotics, 2023. **12**(1): p. 104.
12. Ali, H., et al., Biosynthesis and characterization of cobalt nanoparticles using combination of different plants and their antimicrobial activity. Biosci Rep, 2023. **43**(7).
13. Ma, H., et al., *Size-Dependent Electrochemical Properties of Pure Metallic Nanoparticles.* The Journal of Physical Chemistry C, 2020. **124**(5): p. 3403-3409.
14. Yaqoob, A.A., et al., Recent Advances in Metal Decorated Nanomaterials and Their Various Biological Applications: A Review. Frontiers in Chemistry, 2020. **8**.
15. Amna, R., et al., *26 - Virus detection using nanobiosensors*, in *Nanosensors for Smart Agriculture*, D. Adil, et al., Editors. 2022, Elsevier. p. 547-572.
16. Serenella, M., et al., *An updated overview on metal nanoparticles toxicity.* Seminars in Cancer Biology, 2021. **76**: p. 17-26.
17. Pacurari, M., et al., *A Review on the Respiratory System Toxicity of Carbon Nanoparticles.* International Journal of Environmental Research and Public Health, 2016. **13**(3): p. 325.
18. Braakhuis, H.M., et al., *Progress and future of* in vitro *models to study translocation of nanoparticles.* Arch Toxicol, 2015. **89**(9): p. 1469-95.
19. Crystal, R.G., et al., *Airway epithelial cells: current concepts and challenges.* Proc Am Thorac Soc, 2008. **5**(7): p. 772-7.
20. Ganesan, S., A.T. Comstock, and U.S. Sajjan, *Barrier function of airway tract epithelium.* Tissue Barriers, 2013. **1**(4): p. e24997.
21. Gao, N. and F. Rezaee, Airway Epithelial Cell Junctions as Targets for Pathogens and Antimicrobial Therapy. Pharmaceutics, 2022. **14**(12).
22. Niessen, C.M., Tight junctions/adherens junctions: basic structure and function. J Invest Dermatol, 2007. **127**(11): p. 2525-32.
23. Hiemstra, P.S., P.B. McCray, Jr., and R. Bals, *The innate immune function of airway epithelial cells in inflammatory lung disease.* Eur Respir J, 2015. **45**(4): p. 1150-62.
24. Yuan, J., et al., Effects of metal nanoparticles on tight junction-associated proteins via HIF-1α/miR-29b/MMPs pathway in human epidermal keratinocytes. Particle and Fibre Toxicology, 2021. **18**(1): p. 13.
25. Rotoli, B.M., et al., Non-functionalized multi-walled carbon nanotubes alter the paracellular permeability of human airway epithelial cells. Toxicol Lett, 2008. **178**(2): p. 95-102.
26. Byrne, J.D. and J.A. Baugh, The significance of nanoparticles in particle-induced pulmonary fibrosis. Mcgill J Med, 2008. **11**(1): p. 43-50.
27. Lu, X., et al., *Right or Left: The Role of Nanoparticles in Pulmonary Diseases.* International Journal of Molecular Sciences, 2014. **15**(10): p. 17577-17600.
28. Shah, D.D., et al., Harnessing three-dimensional (3D) cell culture models for pulmonary infections: State of the art and future directions. Naunyn Schmiedebergs Arch Pharmacol, 2023. **396**(11): p. 2861-2880.
29. Frohlich, E. and S. Salar-Behzadi, Toxicological assessment of inhaled nanoparticles: role of in vivo, ex vivo, in vitro, and in silico studies. Int J Mol Sci, 2014. **15**(3): p. 4795-822.
30. Woodrow, J.S., et al., Asthma: The Use of Animal Models and Their Translational Utility. Cells, 2023. **12**(7): p. 1091.
31. Altschuler, S.J. and L.F. Wu, *Cellular heterogeneity: do differences make a difference?* Cell, 2010. **141**(4): p. 559-63.
32. Irvin, C.G. and J.H.T. Bates, *Measuring the lung function in the mouse: the challenge of size.* Respiratory Research, 2003. **4**(1): p. 1.
33. Savage, D.T., J.Z. Hilt, and T.D. Dziubla, In Vitro *Methods for Assessing Nanoparticle Toxicity.* Methods Mol Biol, 2019. **1894**: p. 1-29.
34. Callaghan, P.J., et al., Epithelial barrier function properties of the 16HBE14o- human bronchial epithelial cell culture model. Biosci Rep, 2020. **40**(10).
35. Cozens, A.L., et al., CFTR expression and chloride secretion in polarized immortal human bronchial epithelial cells. Am J Respir Cell Mol Biol, 1994. **10**(1): p. 38-47.

 doi:10.20944/preprints202406.1674.v1

36. Wan, H., et al., Tight junction properties of the immortalized human bronchial epithelial cell lines Calu-3 and 16HBE14o. Eur Respir J, 2000. **15**(6): p. 1058-68.
37. Kerschner, J.L., A. Paranjapye, and A. Harris, Cellular heterogeneity in the 16HBE14o(-) airway epithelial line impacts biological readouts. Physiol Rep, 2023. **11**(11): p. e15700.
38. Garcia, M.A., W.J. Nelson, and N. Chavez, *Cell-Cell Junctions Organize Structural and Signaling Networks.* Cold Spring Harb Perspect Biol, 2018. **10**(4).
39. Wittekindt, O.H., Tight junctions in pulmonary epithelia during lung inflammation. Pflugers Arch, 2017. **469**(1): p. 135-147.
40. Smallcombe, C.C., et al., Titanium dioxide nanoparticles exaggerate respiratory syncytial virus-induced airway epithelial barrier dysfunction. Am J Physiol Lung Cell Mol Physiol, 2020. **319**(3): p. L481-L496.
41. Lee, C.E., et al., 8-Bromo-cAMP attenuates human airway epithelial barrier disruption caused by titanium dioxide fine and nanoparticles. Tissue Barriers, 2024: p. 2300579.
42. Ma, Y., et al., Titanium dioxide nanoparticles induce size-dependent cytotoxicity and genomic DNA hypomethylation in human respiratory cells. RSC Advances, 2017. **7**(38): p. 23560-23572.
43. Guadagnini, R., et al., Toxicity evaluation of engineered nanoparticles for medical applications using pulmonary epithelial cells. Nanotoxicology, 2015. **9 Suppl 1**: p. 25-32.
44. Bao, X. and M. Shi, Toxic effect of silica nanoparticles on bronchial epithelial cells. Materials Express, 2022. **12**(2): p. 255-262.
45. Fu, J., et al., Regulation of c-Myc and Bcl-2 induced apoptosis of human bronchial epithelial cells by zinc oxide nanoparticles. J Biomed Nanotechnol, 2012. **8**(4): p. 669-75.
46. Huo, L., et al., *High-Content Screening for Assessing Nanomaterial Toxicity.* J Nanosci Nanotechnol, 2015. **15**(2): p. 1143-9.
47. Farcal, L., et al., Comprehensive In Vitro Toxicity Testing of a Panel of Representative Oxide Nanomaterials: First Steps towards an Intelligent Testing Strategy. PLoS One, 2015. **10**(5): p. e0127174.
48. Giard, D.J., et al., In vitro cultivation of human tumors: establishment of cell lines derived from a series of solid tumors. J Natl Cancer Inst, 1973. **51**(5): p. 1417-23.
49. Meindl, C., et al., Screening for Effects of Inhaled Nanoparticles in Cell Culture Models for Prolonged Exposure. Nanomaterials (Basel), 2021. **11**(3).
50. Srivastava, R.K., et al., Nano-titanium dioxide induces genotoxicity and apoptosis in human lung cancer cell line, A549. Hum Exp Toxicol, 2013. **32**(2): p. 153-66.
51. Wang, Y., et al., Cytotoxicity, DNA damage, and apoptosis induced by titanium dioxide nanoparticles in human non-small cell lung cancer A549 cells. Environ Sci Pollut Res Int, 2015. **22**(7): p. 5519-30.
52. Chairuangkitti, P., et al., Silver nanoparticles induce toxicity in A549 cells via ROS-dependent and ROS-independent pathways. Toxicol In Vitro, 2013. **27**(1): p. 330-8.
53. Zhuo, L.B., et al., Zinc oxide nanoparticles induce acute lung injury via oxidative stress-mediated mitochondrial damage and NLRP3 inflammasome activation: In vitro and in vivo studies. Environ Pollut, 2024. **341**: p. 122950.
54. Rafieepour, A., et al., The Effect of Particle Size on the Cytotoxicity of Amorphous Silicon Dioxide: An in Vitro Toxicological Study. Asian Pac J Cancer Prev, 2021. **22**(2): p. 325-332.
55. Ren, H., N.P. Birch, and V. Suresh, *An Optimised Human Cell Culture Model for Alveolar Epithelial Transport.* PLoS One, 2016. **11**(10): p. e0165225.
56. Karakocak, B.B., et al., Rethinking of TEER measurement reporting for epithelial cells grown on permeable inserts. Eur J Pharm Sci, 2023. **188**: p. 106511.
57. Peter, Y., et al., Epidermal growth factor receptor and claudin-2 participate in A549 permeability and remodeling: implications for non-small cell lung cancer tumor colonization. Mol Carcinog, 2009. **48**(6): p. 488-97.
58. Braun, N.J., et al., Implementation of a Dynamic Co-Culture Model Abated Silver Nanoparticle Interactions and Nanotoxicological Outcomes In Vitro. Nanomaterials (Basel), 2021. **11**(7).
59. Konczol, M., et al., Cellular uptake and toxic effects of fine and ultrafine metal-sulfate particles in human A549 lung epithelial cells. Chem Res Toxicol, 2012. **25**(12): p. 2687-703.
60. Stearns, R.C., J.D. Paulauskis, and J.J. Godleski, *Endocytosis of ultrafine particles by A549 cells.* Am J Respir Cell Mol Biol, 2001. **24**(2): p. 108-15.
61. Shen, B.Q., et al., Calu-3: a human airway epithelial cell line that shows cAMP-dependent Cl- secretion. Am J Physiol, 1994. **266**(5 Pt 1): p. L493-501.
62. Lee, D.F., M.I. Lethem, and A.B. Lansley, A comparison of three mucus-secreting airway cell lines (Calu-3, SPOC1 and UNCN3T) for use as biopharmaceutical models of the nose and lung. Eur J Pharm Biopharm, 2021. **167**: p. 159-174.
63. Braakhuis, H.M., et al., An Air-liquid Interface Bronchial Epithelial Model for Realistic, Repeated Inhalation Exposure to Airborne Particles for Toxicity Testing. J Vis Exp, 2020(159).
64. Braakhuis, H.M., et al., Transferability and reproducibility of exposed air-liquid interface co-culture lung models. NanoImpact, 2023. **31**: p. 100466.

 doi:10.20944/preprints202406.1674.v1

65. Stuetz, H., et al., The Cultivation Modality and Barrier Maturity Modulate the Toxicity of Industrial Zinc Oxide and Titanium Dioxide Nanoparticles on Nasal, Buccal, Bronchial, and Alveolar Mucosa Cell-Derived Barrier Models. Int J Mol Sci, 2023. **24**(6).
66. George, I., et al., Metallic oxide nanoparticle translocation across the human bronchial epithelial barrier. Nanoscale, 2015. **7**(10): p. 4529-4544.
67. McCarthy, J., et al., Mechanisms of toxicity of amorphous silica nanoparticles on human lung submucosal cells in vitro: protective effects of fisetin. Chem Res Toxicol, 2012. **25**(10): p. 2227-35.
68. Forbes, I.I., Human airway epithelial cell lines for in vitro drug transport and metabolism studies. Pharm Sci Technol Today, 2000. **3**(1): p. 18-27.
69. Foster, K.A., et al., Characterization of the A549 cell line as a type II pulmonary epithelial cell model for drug metabolism. Exp Cell Res, 1998. **243**(2): p. 359-66.
70. Min, K.A., G.R. Rosania, and M.C. Shin, Human Airway Primary Epithelial Cells Show Distinct Architectures on Membrane Supports Under Different Culture Conditions. Cell Biochem Biophys, 2016. **74**(2): p. 191-203.
71. Hiemstra, P.S., T.D. Tetley, and S.M. Janes, *Airway and alveolar epithelial cells in culture.* European Respiratory Journal, 2019. **54**(5): p. 1900742.
72. Zaidman, N.A., A. Panoskaltsis-Mortari, and S.M. O'Grady, Differentiation of human bronchial epithelial cells: role of hydrocortisone in development of ion transport pathways involved in mucociliary clearance. Am J Physiol Cell Physiol, 2016. **311**(2): p. C225-36.
73. Gard, A.L., et al., High-throughput human primary cell-based airway model for evaluating influenza, coronavirus, or other respiratory viruses in vitro. Sci Rep, 2021. **11**(1): p. 14961.
74. Rezaee, F., et al., cAMP-dependent activation of protein kinase A attenuates respiratory syncytial virus-induced human airway epithelial barrier disruption. PLoS One, 2017. **12**(7): p. e0181876.
75. Gao, N., A. Raduka, and F. Rezaee, Respiratory syncytial virus disrupts the airway epithelial barrier by decreasing cortactin and destabilizing F-actin. J Cell Sci, 2022. **135**(16).
76. Kim, I.Y., et al., Comparative Study on Nanotoxicity in Human Primary and Cancer Cells. Nanomaterials (Basel), 2022. **12**(6).
77. Frontinan-Rubio, J., et al., Rapid and efficient testing of the toxicity of graphene-related materials in primary human lung cells. Sci Rep, 2022. **12**(1): p. 7664.
78. Hussain, S., et al., Carbon black and titanium dioxide nanoparticles elicit distinct apoptotic pathways in bronchial epithelial cells. Part Fibre Toxicol, 2010. **7**: p. 10.
79. Ekstrand-Hammarström, B., et al., Human primary bronchial epithelial cells respond differently to titanium dioxide nanoparticles than the lung epithelial cell lines A549 and BEAS-2B. Nanotoxicology, 2012. **6**(6): p. 623-634.
80. Schlinkert, P., et al., The oxidative potential of differently charged silver and gold nanoparticles on three human lung epithelial cell types. J Nanobiotechnology, 2015. **13**: p. 1.
81. Oberdorster, G., et al., Extrapulmonary translocation of ultrafine carbon particles following whole-body inhalation exposure of rats. J Toxicol Environ Health A, 2002. **65**(20): p. 1531-43.
82. Rossi, E.M., et al., Inhalation exposure to nanosized and fine TiO2 particles inhibits features of allergic asthma in a murine model. Part Fibre Toxicol, 2010. **7**: p. 35.
83. Wahle, T., et al., Evaluation of neurological effects of cerium dioxide nanoparticles doped with different amounts of zirconium following inhalation exposure in mouse models of Alzheimer's and vascular disease. Neurochem Int, 2020. **138**: p. 104755.
84. Alqahtani, S., et al., Exacerbation of Nanoparticle-Induced Acute Pulmonary Inflammation in a Mouse Model of Metabolic Syndrome. Front Immunol, 2020. **11**: p. 818.
85. Braakhuis, H.M., et al., Identification of the appropriate dose metric for pulmonary inflammation of silver nanoparticles in an inhalation toxicity study. Nanotoxicology, 2016. **10**(1): p. 63-73.
86. Morimoto, Y., et al., Evaluation of Pulmonary Toxicity of Zinc Oxide Nanoparticles Following Inhalation and Intratracheal Instillation. Int J Mol Sci, 2016. **17**(8).
87. Adamcakova-Dodd, A., et al., Toxicity assessment of zinc oxide nanoparticles using sub-acute and sub-chronic murine inhalation models. Part Fibre Toxicol, 2014. **11**: p. 15.
88. Grassian, V.H., et al., Inflammatory response of mice to manufactured titanium dioxide nanoparticles: Comparison of size effects through different exposure routes. Nanotoxicology, 2007. **1**(3): p. 211-226.
89. Leung, Y.H., et al., *Toxicity of CeO2 nanoparticles – The effect of nanoparticle properties.* Journal of Photochemistry and Photobiology B: Biology, 2015. **145**: p. 48-59.
90. Aalapati, S., et al., Toxicity and bio-accumulation of inhaled cerium oxide nanoparticles in CD1 mice. Nanotoxicology, 2014. **8**(7): p. 786-98.
91. Nemmar, A., et al., The acute pulmonary and thrombotic effects of cerium oxide nanoparticles after intratracheal instillation in mice. Int J Nanomedicine, 2017. **12**: p. 2913-2922.
92. Srinivas, A., et al., Acute inhalation toxicity of cerium oxide nanoparticles in rats. Toxicol Lett, 2011. **205**(2): p. 105-15.

 doi:10.20944/preprints202406.1674.v1

93. Demokritou, P., et al., An in vivo and in vitro toxicological characterisation of realistic nanoscale CeO(2) inhalation exposures. Nanotoxicology, 2013. **7**(8): p. 1338-50.
94. Kim, I.S., M. Baek, and S.J. Choi, Comparative cytotoxicity of Al2O3, CeO2, TiO2 and ZnO nanoparticles to human lung cells. J Nanosci Nanotechnol, 2010. **10**(5): p. 3453-8.
95. Kim, Y.S., et al., Twenty-Eight-Day Repeated Inhalation Toxicity Study of Aluminum Oxide Nanoparticles in Male Sprague-Dawley Rats. Toxicol Res, 2018. **34**(4): p. 343-354.
96. Yousef, M.I., et al., Aluminum oxide and zinc oxide induced nanotoxicity in rat brain, heart, and lung. Physiol Res, 2022. **71**(5): p. 677-694.
97. Larsen, S.T., et al., Airway irritation, inflammation, and toxicity in mice following inhalation of metal oxide nanoparticles. Nanotoxicology, 2016. **10**(9): p. 1254-62.
98. Wan, R., et al., Cobalt nanoparticles induce lung injury, DNA damage and mutations in mice. Part Fibre Toxicol, 2017. **14**(1): p. 38.
99. Hansen, T., et al., Biological tolerance of different materials in bulk and nanoparticulate form in a rat model: sarcoma development by nanoparticles. J R Soc Interface, 2006. **3**(11): p. 767-75.
100. Jeong, J., et al., Response-metrics for acute lung inflammation pattern by cobalt-based nanoparticles. Part Fibre Toxicol, 2015. **12**: p. 13.
101. Lai, X., et al., Intranasal Delivery of Copper Oxide Nanoparticles Induces Pulmonary Toxicity and Fibrosis in C57BL/6 mice. Sci Rep, 2018. **8**(1): p. 4499.
102. Pietrofesa, R.A., et al., Copper Oxide Nanoparticle-Induced Acute Inflammatory Response and Injury in Murine Lung Is Ameliorated by Synthetic Secoisolariciresinol Diglucoside (LGM2605). International Journal of Molecular Sciences, 2021. **22**(17): p. 9477.
103. Kwon, J.-T., et al., Pulmonary Toxicity and Proteomic Analysis in Bronchoalveolar Lavage Fluids and Lungs of Rats Exposed to Copper Oxide Nanoparticles. International Journal of Molecular Sciences, 2022. **23**(21): p. 13265.
104. Linfield, D.T., et al., *Airway tight junctions as targets of viral infections.* Tissue Barriers, 2021. **9**(2): p. 1883965.